

Anomalous dimensions and scalar glueball spectroscopy in AdS/QCD

H. Boschi-Filho, N. R. F. Braga, F. Jugeau, M. A. C. Torres

*Instituto de Física, Universidade Federal do Rio de Janeiro, Caixa Postal 68528,
RJ 21941-972 – Brazil*

E-mails: boschi@if.ufrj.br, braga@if.ufrj.br,
frederic.jugeau@if.ufrj.br, mtorres@if.ufrj.br

ABSTRACT: An extended version of the AdS/QCD Soft-Wall model that incorporates QCD-like anomalous contributions to the dimensions of gauge theory operators is proposed. This approach leads to a relation between scalar glueball masses and beta functions. Using this relation, the glueball mass spectra that emerge from phenomenological QCD beta functions is investigated. The reverse problem is also considered: starting from a linear fit of lattice glueball masses, different possible beta functions are found. Remarkably, some of them present an infrared fixed point at finite coupling.

KEYWORDS: gauge/gravity correspondence, AdS/CFT correspondence, QCD phenomenology.

Contents

1. Introduction	1
2. Scalar Glueballs	3
2.1 Lattice results	3
2.2 The Soft-Wall model in brief	4
2.3 The anomalous dimension of the scalar glueball operator	5
3. Glueball masses from beta functions	6
3.1 Beta function with a cubic IR asymptotic behavior	7
3.2 Beta function with an IR fixed point at finite coupling	8
3.3 Beta function with a linear IR asymptotic behavior	9
4. Effective beta functions from glueball masses	11
4.1 Case $k_1^2 = 16k_2$	13
4.1.1 Solution without change of sign at z_c	13
4.1.2 Solution with change of sign at z_c	14
4.2 Case $k_1^2 < 16k_2$	15
5. Conclusion	18

1. Introduction

The idea that string theory and non-abelian gauge theories are related has been proposed long ago [1]. More recently, an exact equivalence between string theory in ten dimensions and gauge theories in four dimensions was discovered [2, 3, 4]. This relation holds for string theory in $AdS_5 \times S^5$ spacetime and $SU(N)$ Yang Mills theory with large N , extended $\mathcal{N} = 4$ supersymmetry and conformal invariance. This is an example of the AdS/CFT correspondence which also includes other gauge/string dualities in different geometries and dimensions.

In order to apply the idea of gauge/gravity dualities to describe strong interactions, it is necessary to break the conformal invariance. Presently, an exact dual description of QCD is not known. However, in the recent years, some important QCD properties have been reproduced from phenomenological models based on the AdS/CFT correspondence. Essentially, these so called AdS/QCD models consist in modifying the AdS geometry with the purpose of breaking the conformal invariance.

An infrared scale in the gauge theory was associated with a localization in the AdS space in Ref.[5]. This way a physical process with an infrared scale in four dimensions is mapped into a region of the AdS space. Using this idea, the correct high energy scaling of hadronic amplitudes for fixed angle scattering was found. This experimentally observed scaling was reproduced by QCD long before in [6, 7, 8].

Putting forward the idea of Ref.[5] to relate AdS/CFT and QCD, in Ref. [9, 10] the scalar glueball spectroscopy was studied using an AdS slice. The size of the slice is related to Λ_{QCD} . Considering boundary conditions in the AdS slice, normalizable modes for the scalar bulk fields dual to scalar glueballs with a discrete spectrum were found. The approach of using an AdS slice to investigate hadronic properties was then called AdS/QCD Hard-Wall model and applied to other particles (see *e.g* [11]).

It was then realized that the Regge trajectories that can be obtained from the Hard-Wall model are not linear. Then, another AdS/QCD model was proposed to give linear trajectories, especially for vector mesons. This was done with the introduction of a dilaton background field that plays the role of a smooth cut-off in the AdS spacetime [12]. This is called Soft-Wall model and was also applied to study scalar particle properties [13, 14, 15, 16].

Another interesting approach to the holographic description of QCD appeared in [17, 18] (see also [19] for a review). In these models, dilaton potentials are related to QCD beta functions. This makes it possible to use these holographic models to obtain many QCD properties. In particular, they obtained glueball masses in agreement with lattice results.

In the AdS/CFT correspondence, the masses of supergravity fields are related to the scaling dimension of the local gauge-invariant dual operators. Since the gauge theory is conformal, the beta function vanishes. So, the scaling dimensions of the operators do not get anomalous contribution keeping their canonical dimensions. In the original AdS/QCD models, one usually assumes that the relation between the masses of the bulk fields and the scaling dimension of the boundary operators is the same as in the AdS/CFT correspondence.

The purpose of this work is to study the scalar glueball mass spectrum taking into account contributions from the anomalous dimension of the glueball operator in a Soft-Wall background. This anomalous dimension implies a modification of the mass of the dual five dimensional supergravity field. This modification implies in turn a correction on the four dimensional mass spectrum. We study the case of the scalar glueballs, that are dual to scalar bulk fields in the holographic AdS spacetime.

We consider some possible phenomenological beta functions and find the corresponding glueball mass spectra. We also investigate the inverse problem: starting from a linear fit of lattice quadratic glueball masses, we identify possible corresponding beta functions.

The paper is organized as follows. In section 2, we review lattice results, discuss the Soft-Wall model and calculate the anomalous dimension of the scalar glueball

operator. In section 3, we obtain glueball spectra from three different beta functions considered in the literature. Section 4 is devoted to constructing beta functions able to reproduce linear Regge trajectories of lattice scalar glueball masses.

2. Scalar Glueballs

2.1 Lattice results

The glueball mass spectrum has been the subject of numerous studies in lattice QCD [20, 21, 22, 23], which have provided estimates for the groundstate and a few excited states as shown in Table 1 (for general reviews, see for instance [24, 25]).

	Ref. [20]	Ref. [21]	Ref. [22]	Ref. [23]	
J^{PC}	$N_c = 3$	$N_c = 3$, anisotropic lattice		$N_c = 3$	$N_c \rightarrow \infty$
0^{++}	1.475(30)(65)	1.730(50)(80)	1.710(50)(80)	1.58(11)	1.48(07)
0^{+++}	2.755(70)(120)	2.670(180)(130)		2.75(35)	2.83(22)
0^{++**}	3.370(100)(150)				
0^{++++}	3.990(210)(180)				

Table 1: Lattice scalar glueball mass spectra in GeV. The errors are shown in parenthesis and described in the text.

In the second column, we show the results of Ref.[20] computed for pure $SU(3)_c$ lattice gauge theory. The first number in parenthesis is the statistical error stemming from the continuum-limit extrapolation while the second error accounts for the uncertainty in the string tension σ .

In the third and fourth columns of Table 1, we show results from Refs.[21, 22] where anisotropic lattices have been used with different temporal and spatial spacings. The first error comes from the combined uncertainties from the continuum-limit extrapolation and from the anisotropy, the second from the uncertainty in a hadronic length scale playing a role similar to the string tension.

It is worth pointing out that most of the investigations in lattice consider $SU(N_c)$ theories at finite N_c . However, in the AdS/CFT correspondence, the Yang-Mills theory is in the large N_c limit. In order to compare the large- N_c gauge theory to its finite counterpart, Ref.[23] calculated the lightest and the first excited scalar glueball masses in gauge theories for increasing N_c and it was found a mass difference for the glueballs of about only 5% between the $N_c = 3$ and the large- N_c gauge theories (see also [26]). These results are shown in the last two columns of Table 1 where we used the mean value $\sqrt{\sigma} = 440$ MeV of [20].

2.2 The Soft-Wall model in brief

The AdS/QCD Soft-Wall model is defined by the action [12]:

$$S = \int d^5x \sqrt{-g} e^{-\Phi} \mathcal{L} , \quad (2.1)$$

where \mathcal{L} is the Lagrangian density, Φ is the static background dilaton field and g is the determinant of the metric tensor of AdS_5 , given by

$$ds^2 \equiv g_{mn} dx^m dx^n = \frac{R^2}{z^2} (\eta_{\mu\nu} dx^\mu dx^\nu + dz^2) , \quad (2.2)$$

with $\eta_{\mu\nu} = (-, +, +, +)$ the Minkowski $4d$ metric. R is the AdS_5 radius and z is the holographic coordinate allowed to run from zero to infinity. In the following, we will set $R = 1$ as it does not enter expressions of any four dimensional physical quantity as particle masses. In this model, the infrared cut-off is represented by a background dilaton field chosen as $\Phi = cz^2$ where the dilaton parameter c has the dimension of a squared mass.

For the case of a massive scalar bulk field $X = X(x, z)$, the action takes the form [13]:

$$S = \int d^5x \sqrt{-g} e^{-\Phi(z)} [g^{mn} \partial_m X \partial_n X + m_{AdS}^2 X^2] \quad (2.3)$$

and the equation of motion is

$$\partial_z \left(\frac{1}{z^3} e^{-\Phi(z)} \partial_z X \right) + \frac{1}{z^3} e^{-\Phi(z)} \eta^{\mu\nu} \partial_\mu \partial_\nu X - \frac{1}{z^5} e^{-\Phi(z)} m_{AdS}^2 X = 0 . \quad (2.4)$$

Representing the scalar field through a $4d$ Fourier transform:

$$X(x, z) = \int \frac{d^4q}{(2\pi)^4} e^{iq \cdot x} \tilde{X}(q, z) ,$$

one has:

$$\partial_z (e^{-B(z)} \partial_z \tilde{X}) - q^2 e^{-B(z)} \tilde{X} - \frac{m_{AdS}^2}{z^2} e^{-B(z)} \tilde{X} = 0 \quad (2.5)$$

with $B(z) = \Phi(z) + 3 \ln(z)$. Under the change of function $\tilde{X} = e^{B/2} \tilde{Y}$, one finally gets a $1d$ Schrödinger-like equation:

$$-\partial_z^2 \tilde{Y} + V(z) \tilde{Y} = -q^2 \tilde{Y} \quad (2.6)$$

with the $5d$ effective potential:

$$V(z) = \frac{B'^2}{4} - \frac{B''}{2} + \frac{m_{AdS}^2}{z^2} = c^2 z^2 + \frac{15}{4z^2} + 2c + \frac{m_{AdS}^2}{z^2} . \quad (2.7)$$

The normalizable solutions of Eq.(2.6) correspond to a discrete spectrum of $4d$ masses $q_n^2 \equiv -m_n^2$. The $5d$ mass is related to the scaling dimension Δ of the dual $4d$ boundary operator as

$$m_{AdS}^2 = \Delta(\Delta - 4) . \quad (2.8)$$

The scalar glueball is associated with the local gauge-invariant QCD operator $tr(G_{\mu\nu}G^{\mu\nu})$ defined on the boundary spacetime and which has classical dimension $\Delta_{class.} = 4$ implying then $m_{AdS} = 0$. The corresponding mass spectrum was found in [13]:

$$m_{G_n}^2 = 4c(n+2) . \quad (2.9)$$

If one fixes c by the mass spectrum of the vector ρ mesons in AdS/QCD as $c = 0.2325 \text{ GeV}^2 = (0.482 \text{ GeV})^2$ [12], one obtains the results shown in Table 2.

0^{++}	0^{+++}	0^{++++}	0^{+++++}
1.364	1.670	1.929	2.566

Table 2: Scalar glueball masses in GeV from the Soft-Wall model [13].

One points out that these results from the Soft-Wall model are systematically smaller than the lattice values of glueball masses reviewed in the previous subsection. Furthermore, it is interesting to note that even changing the value of c , one can not fit the lattice glueball masses using the relation (2.9).

We will see how these masses can be increased by the introduction of the anomalous contribution to the dimension of the scalar glueball operator. The anomalous dimension coming from quantum effects depends on the renormalization scale μ of the four dimensional boundary theory. On the other side, holography implies that the fifth z coordinate representing the energy scale at which physical processes occur is inversely proportional to μ [27]. So, the bulk mass (2.8) with Δ the full dimension will depend on the z coordinate, thus acting as an additional effective potential for the Schrödinger-like equation (2.6).

2.3 The anomalous dimension of the scalar glueball operator

We calculate the full dimension of the scalar glueball operator in our phenomenological holographic model inspired by QCD. For this, following [28], we consider the trace anomaly of the QCD energy-momentum tensor:

$$T^\mu_\mu = \frac{\beta(\alpha)}{16\pi\alpha^2} tr G^2 + \text{fermionic terms} \quad (2.10)$$

where the beta function is defined as usual as

$$\beta(\alpha(\mu)) \equiv \frac{d\alpha(\mu)}{d\ln(\mu)} \quad (2.11)$$

with $\alpha \equiv g_{YM}^2/4\pi$ and g_{YM} the Yang-Mills coupling constant.

On the other hand, for any operator \mathcal{O} , we have the following scaling behaviour:

$$\Delta_{\mathcal{O}} \mathcal{O} = - \frac{d\mathcal{O}}{d\ln \mu} \quad (2.12)$$

where the full dimension $\Delta_{\mathcal{O}} = \Delta_{class.} + \gamma(\mu)$ is given in terms of the classical dimension $\Delta_{class.}$ and the anomalous dimension $\gamma(\mu)$. In the following, the fermionic contribution on the *r.h.s* of (2.10) will not be considered, since we are interested only in the equation for the operator $tr G^2$. Thus, by taking into account the scalar glueball operator contribution of the QCD trace anomaly, Eq.(2.12) gives:

$$\begin{aligned}\Delta_{T_\mu^\mu} \left(\frac{\beta(\alpha)}{8\pi\alpha^2} tr G^2 \right) &= -\frac{d}{d \ln \mu} \left(\frac{\beta(\alpha)}{8\pi\alpha^2} tr G^2 \right) \\ &= -(\beta'(\alpha) - \frac{2}{\alpha}\beta(\alpha) - \Delta_{G^2}) \frac{\beta(\alpha)}{8\pi\alpha^2} tr G^2\end{aligned}\quad (2.13)$$

where the prime denotes the derivative with respect to α . The trace T_μ^μ scales classically, that means $\Delta_{T_\mu^\mu} = 4$. This finally implies that the scalar glueball operator $tr G^2$ has the full dimension:

$$\Delta_{G^2} = 4 + \beta'(\alpha) - \frac{2}{\alpha}\beta(\alpha) . \quad (2.14)$$

From now on, we will express the beta function in terms of the 't Hooft coupling $\lambda \equiv N_c g_{YM}^2 = 4\pi N_c \alpha$ and the prime will now denote derivative with respect to λ . The anomalous dimension defined above implies a correction for the bulk mass so that the potential (2.7) becomes

$$V(z) = c^2 z^2 + \frac{15}{4z^2} + 2c + \frac{1}{z^2} \left[4 + \beta'(\lambda) - \frac{2}{\lambda}\beta(\lambda) \right] \left[\beta'(\lambda) - \frac{2}{\lambda}\beta(\lambda) \right] . \quad (2.15)$$

In the following, we will solve the 1d Schrödinger-like equation (2.6) with this generalized potential for different beta functions and determine the corresponding glueball mass spectra.

3. Glueball masses from beta functions

In this section, we will consider some beta functions discussed in the literature [29, 30] and adjust their different parameters in order - if possible - to obtain a mass spectrum compatible with the glueball lattice results. We will also demand that the various beta functions have a ultraviolet perturbative behaviour similar to QCD for small λ at 1-loop order:

$$\beta(\lambda) \approx -b_0 \lambda^2 , \quad (3.1)$$

where b_0 is a positive constant in order to guarantee the asymptotic freedom property of QCD.

Note that the *r.h.s.* of Eq.(3.1) was considered in [29] as an attempt for a beta function when investigating the heavy quark-antiquark interaction potential in some Renormalization Group revised AdS/QCD models. However, in our phenomenological framework, such a beta function can not give additional anomalous contribution

to the effective potential, since the last term in (2.15) vanishes identically in this case.

In the holographic models of QCD, the energy scale is related to the fifth coordinate of the AdS space by $\mu = 1/z$. Hence, we can write an equation for the beta function in terms of z as

$$\mu \frac{d\lambda(\mu)}{d\mu} = \beta(\lambda(\mu)) \Rightarrow z \frac{d\lambda(z)}{dz} = -\beta(\lambda(z)) . \quad (3.2)$$

We will choose the value of $\lambda(z_0) \equiv \lambda_0$ at the energy scale given by the mass M_{Z^0} of the neutral Z^0 boson so that

$$z_0 \equiv 1/M_{Z^0} = 0.010966 \text{ GeV}^{-1} \quad (3.3)$$

and corresponding to the world average value of the strong coupling [31]:

$$\alpha_s = 0.1184 \Rightarrow \lambda_0 = 4.464 \quad (N_c = 3) . \quad (3.4)$$

3.1 Beta function with a cubic IR asymptotic behavior

First, let us consider the following beta function [29]:

$$\beta(\lambda) = -b_0\lambda^2 - b_1\lambda^3 \quad (b_0, b_1 > 0) . \quad (3.5)$$

This beta function behaves as $-\lambda^3$ in the infrared.

In this case, the renormalization group equation can be exactly solved, finding

$$z(\lambda) = z_0 e^{\frac{1}{b_0} \left(\frac{1}{\lambda_0} - \frac{1}{\lambda} \right)} \left(\frac{b_1\lambda + b_0}{b_1\lambda_0 + b_0} \frac{\lambda_0}{\lambda} \right)^{b_1/b_0^2} \quad (3.6)$$

where $\lambda(z_0) = \lambda_0$ fixes the integration constant.

On the one hand, when $\lambda \ll 1$, we recover, as it must be, a QCD-like behaviour:

$$\lambda(z) \simeq \frac{1}{b_0 \ln\left(\frac{z_0}{z} e^{1/b_0\lambda_0}\right)} \quad (3.7)$$

at the leading order. On the other hand, the limit $\lambda \rightarrow \infty$ is reached for a finite value of z given by

$$z_{max} = \frac{z_0 e^{\frac{1}{b_0\lambda_0}}}{\left(1 + \frac{b_0}{b_1\lambda_0}\right)^{b_1/b_0^2}} . \quad (3.8)$$

This beta function implies that the potential of Eq.(2.15) takes the form:

$$V(z) = c^2 z^2 + \frac{15}{4z^2} + 2c - \frac{1}{z^2} b_1 \lambda(z)^2 (4 - b_1 \lambda(z)^2) . \quad (3.9)$$

So, in contrast with the Soft-Wall model, $V(z)$ goes to infinity at $z = z_{max}$. In other words, there is an infinite wall located at z_{max} and the solutions of the

Schrödinger like equation will be non-vanishing only in the region $0 < z < z_{max}$. As an unexpected consequence, the beta function (3.5) leads to the formation of a hard wall in the $5d$ effective potential. The fact that the background was initially of the Soft-Wall model does not have significant influence in getting the glueball mass spectrum in this case, as shown in Table 3 where a vanishing dilaton parameter c is in fact a quite acceptable value.

In order to do the numerical analysis for this beta function, we employ a standard shooting method and assume that the ratio between b_0 and b_1 follows the perturbative relation $b_1 = (51/121)b_0^2$ valid for pure $SU(3)_c$ gauge theory [18, 32]. So, we will consider c and b_0 as the independent parameters of the model. We use these parameters to fit the first two isotropic lattice glueball masses within their uncertainty ranges [20] given in Table 1. Then, we calculate the other masses and compare them with the third and fourth masses listed in Table 1. It appears a lower bound for b_0 below which there is no value of c able to match the mass spectrum. When b_0 attains its lower bound $b_0^{(min)} = 0.03244$, only the value of $c = (0.385 \text{ GeV})^2$ allows us to fit the masses shown in the first row of Table 3.

Increasing the value of b_0 , we find a range of possible values for c . For example, for $b_0 = 0.03250$, we can fit the first two masses by considering values in the interval $0.300 \leq \sqrt{c} \leq 0.366 \text{ GeV}$. For $b_0 = 0.03270$, we find the interval $0 \leq \sqrt{c} \leq 0.27 \text{ GeV}$. We also find that for $c = 0$, we can fit the first two masses provided that $0.03258 \leq b_0 \leq 0.03290$. For the sake of illustration, in the last two rows of Table 3 we show the mass spectra for the mean values of \sqrt{c} and b_0 corresponding to the ranges associated respectively with $b_0 = 0.03250$ and $c = 0$. Finally, note that the values found for b_0 are relatively close to the perturbative $b_0^{(pert)1}$.

b_0	\sqrt{c}	z_{max}	0^{++}	0^{++*}	0^{++++}	0^{++++}
0.03244	0.385	3.286	1.570	2.567	3.545	4.518
0.03250	0.330	3.247	1.546	2.574	3.570	4.559
0.03270	0.000	3.120	1.515	2.625	3.677	4.714

Table 3: Masses for the scalar glueball groundstate and the excitations $J^{PC} = 0^{++}$ for the beta function with a cubic IR asymptotic behavior for different values of b_0 and c . Masses and \sqrt{c} are expressed in GeV. For completeness, we also show the values of z_{max} expressed in GeV^{-1} .

3.2 Beta function with an IR fixed point at finite coupling

The beta function:

$$\beta(\lambda) = -b_0 \lambda^2 \left(1 - \frac{\lambda}{\lambda_*} \right) \quad (\lambda_* > 0) \quad (3.10)$$

¹For instance, $b_0^{(pert)} \simeq 0.03237$ for $n_f = 5$.

reproduces the perturbative $\beta(\lambda) \sim -b_0\lambda^2$ at 1-loop order in the ultraviolet and behaves as $\beta(\lambda) \sim +\lambda^3$ in the infrared. This beta function has been used for instance in Ref.[30]. Solving Eq.(3.2) for the beta function (3.10), we find:

$$z(\lambda) = C e^{-\frac{1}{b_0\lambda}} e^{\frac{1}{b_0\lambda_*} \ln(\frac{\lambda}{|\lambda-\lambda_*|})} \quad (3.11)$$

where C is an integration constant. Note that there are two solutions, one for $\lambda > \lambda_*$ and another for $\lambda < \lambda_*$. In the first case, the solution does not show asymptotic freedom. So, we will consider only the physically relevant case $\lambda < \lambda_*$ for which we fix C imposing $\lambda(z_0) \equiv \lambda_0$ and we finally obtain:

$$z(\lambda) = z_0 e^{\frac{1}{b_0}(\frac{1}{\lambda_0} - \frac{1}{\lambda})} \left(\frac{\lambda_* - \lambda_0}{\lambda_* - \lambda} \frac{\lambda}{\lambda_0} \right)^{\frac{1}{b_0\lambda_*}} \quad (3.12)$$

where the values of z_0 and λ_0 are given in Eqs.(3.3) and (3.4). In particular, for $\lambda \ll 1$, we recover the QCD asymptotic behavior of Eq.(3.7).

Writing λ as a function of z and substituting into the beta function and then in the potential (2.15), we solve numerically the corresponding Schrödinger equation to find the glueball masses. The masses depend on the parameters: b_0 , c and λ_* . For this case, we did not find a reasonable set of parameters that fits the masses for the isotropic lattice [20], the reason being essentially the gap between the groundstate and the first excited state (around 1.3 GeV, to be compared with the smaller gap of 0.94 GeV for anisotropic lattice [21]). However, for the anisotropic lattice results [21], we can fit the first two masses with the choice $b_0 = 0.091$, $\sqrt{c} = 0.55$ GeV and $\lambda_* = 600$. These results and also the predictions for the third and fourth excited states are shown in Table 4. It is interesting to remark that we can still fit the first two masses keeping two of these parameters with the values shown above and varying the third one in the intervals: $0.03902 \leq b_0 \leq 0.04005$, $0.535 \leq \sqrt{c} \leq 0.616$, GeV and $\lambda_* \geq 552$. The ranges of values for b_0 and \sqrt{c} turn out to be rather stringent. As for the lower bound on λ_* , it allows the IR fixed point to be pushed away to infinity, giving rise then to a beta function with a fixed point at infinite coupling. Such beta functions have been considered, for instance, in [17].

b_0	\sqrt{c}	λ_*	0^{++}	0^{++*}	0^{++++}	0^{++++*}
0.0391	0.55	600	1.734	2.380	3.053	3.727

Table 4: Masses for the scalar glueball states for the beta function with an IR fixed point at finite coupling. Masses and \sqrt{c} expressed in GeV.

3.3 Beta function with a linear IR asymptotic behavior

Now we consider the following beta function [29, 33]:

$$\beta(\lambda) = -\frac{b_0\lambda^2}{1 + b_1\lambda} \quad (b_0, b_1 > 0) \quad (3.13)$$

that behaves like the perturbative QCD beta function at 1-loop order and decreases asymptotically as $-\lambda$ in the infrared.

In this case, the 5d effective potential reads:

$$V(z) = c^2 z^2 + \frac{15}{4z^2} + 2c + \frac{1}{z^2} \frac{b_0 b_1 \lambda(z)^2 [4(1 + b_1 \lambda(z))^2 + b_0 b_1 \lambda(z)^2]}{(1 + b_1 \lambda(z))^4} \quad (3.14)$$

and the solution of the renormalization group equation is

$$\lambda(z) = \frac{1}{b_1 W \left(\frac{e^{\frac{1}{b_1 \lambda_0}}}{b_1 \lambda_0} \left(\frac{z_0}{z} \right)^{b_0/b_1} \right)} \quad (3.15)$$

where $W(x)$ is the Lambert function (satisfying the property $W(x)e^{W(x)} = x$) and the integration constant is fixed such that $\lambda(z_0) = \lambda_0$. The potential can then be put into the form:

$$V(z) = c^2 z^2 + \frac{15}{4z^2} + 2c + \frac{1}{z^2} \frac{b_0}{b_1} \frac{\left[4 \left(1 + W \left(\frac{e^{\frac{1}{b_1 \lambda_0}}}{b_1 \lambda_0} \left(\frac{z_0}{z} \right)^{b_0/b_1} \right) \right)^2 + \frac{b_0}{b_1} \right]}{\left[1 + W \left(\frac{e^{\frac{1}{b_1 \lambda_0}}}{b_1 \lambda_0} \left(\frac{z_0}{z} \right)^{b_0/b_1} \right) \right]^4}. \quad (3.16)$$

In the infrared limit (when z is large), the coupling constant behaves as $\lambda(z)|_{z \gg z_0} \sim z^{b_0/b_1}$ such that

$$V(z)|_{z \gg z_0} \sim c^2 z^2 + \frac{15}{4z^2} + 2c + \frac{b_0(4b_1 + b_0)}{b_1^2} \frac{1}{z^2}. \quad (3.17)$$

In other words, when $z \rightarrow \infty$, the potential contribution stemming from the anomalous dimension is subleading with respect to the oscillator-like term $c^2 z^2$ coming from the soft wall background dilaton field. Consequently, the Regge-like behaviour of the mass spectrum $m_n^2 \sim n$ for large n is not modified, in contrast to the case of the beta function with a cubic IR asymptotic behavior (cf. subsection 3.1) which led instead to a hard wall-like mass spectrum $m_n^2|_{n \gg 1} \sim n^2$.

The masses depend on the parameters: b_0 , b_1 and c . Once again, we have not been able to find a reasonable set of parameters that fits the masses for the isotropic lattice but, as for the anisotropic lattice results, we can fit the first two masses with the choice $b_0 = 0.0395$, $\sqrt{c} = 0.49$ GeV and $b_1 = 0.001$. These results and also the predictions for the third and fourth states are shown in Table 5. The first two masses can still be fitted keeping two of these parameters with the values shown above while varying the third one within the intervals: $0.0391 \leq b_0 \leq 0.0404$, $0.396 \leq \sqrt{c} \leq 0.593$ GeV, and $0 < b_1 \leq 0.00156$. When b_1 goes to zero, the potential presents the form of a very deep and sharp well mimicking a hard wall-like potential, at least for the lowest-excited states.

b_0	\sqrt{c}	b_1	0^{++}	0^{++*}	0^{++++}	0^{++++*}
0.0395	0.49	0.001	1.704	2.485	3.285	4.096

Table 5: Glueball masses in GeV for the the beta function (3.13). \sqrt{c} is expressed in GeV whereas b_0 and b_1 are dimensionless.

4. Effective beta functions from glueball masses

The glueball masses obtained from lattice studies shown in Table 1 lie approximately in linear Regge trajectories, namely, the square of the masses has approximately a linear relation with the radial quantum number. In this section, we build up beta functions that reproduce this behaviour. In particular, we will consider the masses from the isotropic lattice calculations shown in the second column of Table 1. A linear fit for these masses corresponds to

$$m_n^2 = 4.50n + 2.51, \quad (4.1)$$

where the masses squared are given in GeV^2 . This linear fit implies the glueball masses given in Table 6. The first mass is just 1% above the lattice result including the error bar. The other three masses are within the error bars.

0^{++}	0^{++*}	0^{++++}	0^{++++*}
1.585	2.648	3.393	4.001

Table 6: Glueball masses in GeV from the linear fit of Eq.(4.1).

In order to obtain the class of beta functions that lead to this Regge linear spectrum, we consider the soft-wall potential modified by the contributions from the anomalous dimension of the scalar glueball operator (2.15):

$$V(z) = c^2 z^2 + \frac{15}{4z^2} + 2c + \frac{1}{z^2} [4 + f(z)] f(z) \quad (4.2)$$

where

$$f(z) \equiv \frac{d\beta(\lambda)}{d\lambda} - \frac{2}{\lambda} \beta(\lambda). \quad (4.3)$$

It is convenient to rewrite $f(z)$ in terms of the coupling $\lambda(z)$:

$$\begin{aligned} f(z) &= -1 - z \left(\frac{\lambda''}{\lambda'} - 2 \frac{\lambda'}{\lambda} \right) \\ &= -1 - z \frac{d}{dz} \left(\ln \frac{\lambda'}{\lambda^2} \right) \end{aligned} \quad (4.4)$$

where prime denotes derivative with respect to z .

We use the following ansatz

$$(f(z) + 2)^2 = k + k_1 z^2 + k_2 z^4, \quad (4.5)$$

where k , k_1 and k_2 are constants. The above ansatz requires the positivity condition

$$k_1^2 \leq 4kk_2. \quad (4.6)$$

The potential takes the form

$$V(z) = (c^2 + k_2) z^2 + \frac{k - \frac{1}{4}}{z^2} + (2c + k_1) \quad (4.7)$$

Solving the Schrödinger equation (2.6) with this potential for $k = m^2$ where m is an integer, one finds the $4d$ mass spectrum:

$$m_n^2 = 4\sqrt{c^2 + k_2} n + 2\sqrt{c^2 + k_2}(m + 1) + 2c + k_1. \quad (4.8)$$

This equation can be matched to the glueball linear fit of Eq.(4.1). This matching and the positivity condition (4.6) determine the allowed ranges of the parameters k_1 , k_2 , c , and m . It turns out that $c_{min} \leq c \leq c_{max}$ where

$$c_{min} = -(0.983 \text{ GeV})^2 \quad ; \quad c_{max} = (0.344 \text{ GeV})^2. \quad (4.9)$$

The extreme values of c saturate the positivity condition, *i.e.*, $k_1^2 = 4kk_2$. We also observe that k_1 takes only negative values.

Let us now determine the corresponding beta functions. From Eqs.(4.4) and (4.5), we have to solve the differential equation:

$$\frac{d}{dz} \ln \left(\frac{\lambda'(z)}{\lambda^2(z)} \right) = \frac{1}{z} \mp \frac{1}{z} \sqrt{k + k_1 z^2 + k_2 z^4} \quad (4.10)$$

To reproduce QCD asymptotic behaviour at leading order shown in Eq.(3.7), we impose that

$$\lim_{z \rightarrow 0} \left(\frac{1}{\lambda(z)} \right)' = -\frac{b_0}{z}, \quad (4.11)$$

which implies:

$$\lim_{z \rightarrow 0} \frac{d}{dz} \ln \left(\frac{\lambda'(z)}{\lambda^2(z)} \right) = -\frac{1}{z}. \quad (4.12)$$

Then we must have $k = 4$ (and $m = 2$). For small z , we also must take the upper sign in Eq.(4.10). Note that this analysis of the perturbative small z limit does not impose the sign of Eq.(4.10) for large values of z as it will be discussed below.

We will treat separately the cases $k_1^2 = 16k_2$ and $k_1^2 < 16k_2$, since then the differential equation (4.10) assumes different forms.

4.1 Case $k_1^2 = 16k_2$

In this case, c can take any one of the two values c_{min} and c_{max} . Then, the ansatz (4.5) and the differential equation (4.10) together with (4.4) reduces to:

$$1 - z \frac{d}{dz} \left(\ln \frac{\lambda'}{\lambda^2} \right) = \pm (2 + \frac{k_1}{4} z^2) . \quad (4.13)$$

Since k_1 is negative, there is a critical value of z given by $z_c^2 = -8/k_1$, such that the *r.h.s.* of Eq.(4.13) is zero. We get $z_c = 1.8615 \text{ GeV}^{-1}$ and $z_c = 1.337 \text{ GeV}^{-1}$ for $c = c_{min}$ and $c = c_{max}$, respectively. For $z < z_c$, the sign of (4.13) is fixed by the perturbative limit. For $z \geq z_c$ we are free to choose the sign, without spoiling the smoothness of the coupling $\lambda(z)$. In the following, we are going to consider the two possibilities.

4.1.1 Solution without change of sign at z_c

We take the upper sign of (4.13) for all values of z and find an analytical solution:

$$\lambda(z) = \frac{\lambda_0}{1 - b_0 \frac{\lambda_0}{2} [Ei(-\frac{k_1}{8} z^2) - Ei(-\frac{k_1}{8} z_0^2)]} \quad (4.14)$$

where $Ei(x)$ is the exponential integral function and the initial condition $\lambda(z_0) = \lambda_0$ has been used. We assume from now on that b_0 takes its perturbative expression with $N_c = 3$:

$$b_0 = \frac{1}{8\pi^2} \left(\frac{11}{3} - \frac{2n_f}{9} \right) . \quad (4.15)$$

This equation introduces the number of flavours n_f . However, the four lattice glueball masses that we use in this section were obtained from $SU(3)_c$ with no flavour. Note that unquenched lattice QCD only provides the ground-state scalar glueball mass, usually suffering from severe computational difficulties (lack of high statistics, coarse lattice spacing, etc) [34, 35, 36, 37]. By varying n_f in the coupling (4.14) we will describe effectively the infrared contribution in b_0 appearing in (4.11). We will see in the following that the low energy behaviour of the coupling changes according to n_f .

The beta function for this particular case reads:

$$\beta(z) \equiv -z\lambda'(z) = - \frac{\lambda_0^2 b_0 e^{-\frac{k_1}{8} z^2}}{\left\{ 1 - b_0 \frac{\lambda_0}{2} [Ei(-\frac{k_1}{8} z^2) - Ei(-\frac{k_1}{8} z_0^2)] \right\}^2} . \quad (4.16)$$

Considering the two possible values for c which fixes k_1 and k_2 , we have plotted in Figure 1 the couplings and the beta functions in terms of the holographic coordinate z for $n_f = 0, 3$ and 6. Both $\lambda(z)$ and $\beta(z)$ diverge at a finite value of $z = z_{max}$ where the denominators in (4.14) and (4.16) vanish. Note that z_{max} depends on n_f . In Figure 2, we show the dependence of the beta functions on the coupling λ for these two values of c .

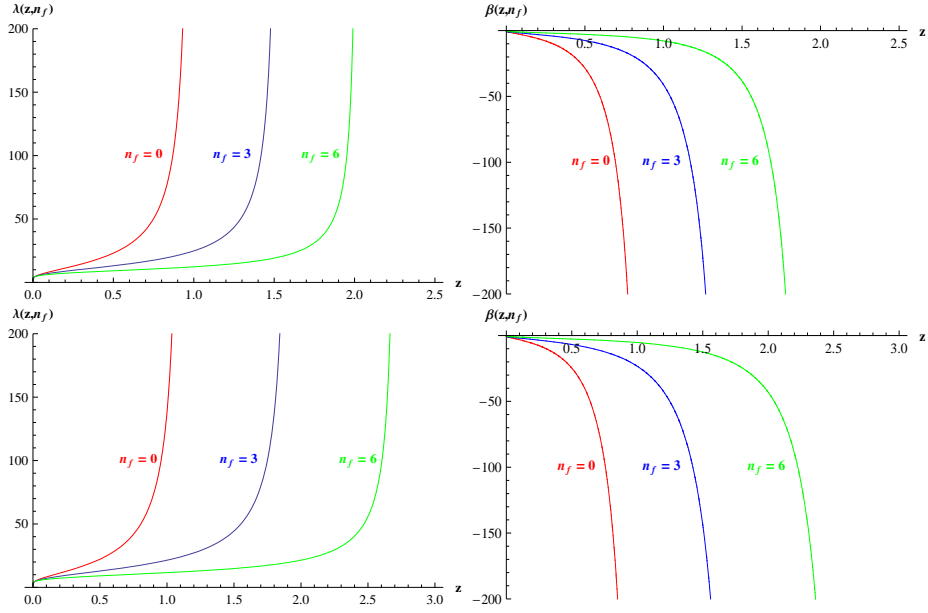


Figure 1: The 't Hooft couplings $\lambda(z)$ and the effective beta functions $\beta(z)$ as a function of z as defined in Eqs.(4.14) and (4.16) for different values of n_f and $c = c_{max}$ (upper panels) and $c = c_{min}$ (lower panels).

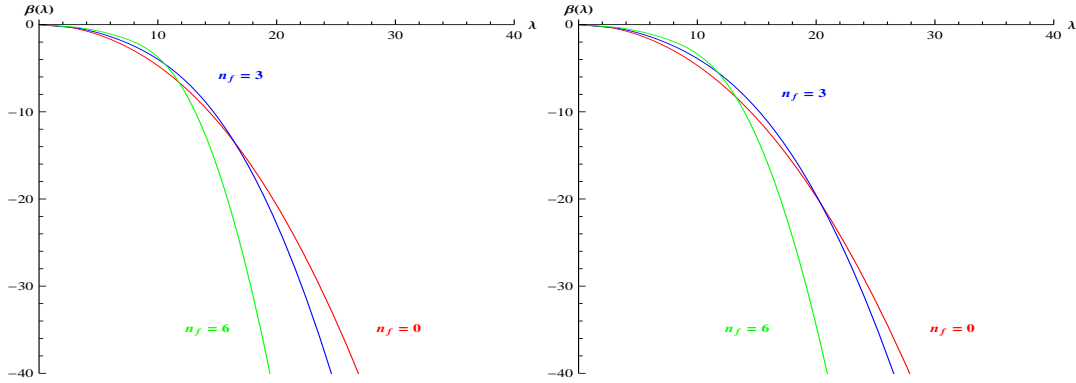


Figure 2: The effective beta function $\beta(\lambda)$ in terms of λ for different values of n_f when $c = c_{max}$ (left) and $c = c_{min}$ (right).

4.1.2 Solution with change of sign at z_c

Now we choose for the differential equation (4.13) the following form

$$z \frac{d}{dz} \left(\ln \frac{\lambda'}{\lambda^2} \right) = \begin{cases} -(1 + \frac{k_1}{4} z^2) & z < z_c, \\ (3 + \frac{k_1}{4} z^2) & z \geq z_c. \end{cases} \quad (4.17)$$

The solution is

$$\lambda(z) = (1 - \Theta(z - z_c)) \lambda_<(z) + \frac{\Theta(z - z_c)}{\frac{1}{\lambda_<(z_c)} + \frac{b_0}{2} \left(\frac{z^2}{z_c^2} + 1 \right) e^{2 - \frac{z^2}{z_c^2}} - b_0 e}, \quad (4.18)$$

yielding the beta function:

$$\beta(z) = (1 - \Theta(z - z_c)) \beta_<(z) - \frac{\Theta(z - z_c)}{\left[\frac{1}{\lambda_<(z_c)} + \frac{b_0}{2} \left(\frac{z^2}{z_c^2} + 1 \right) e^{2 - \frac{z^2}{z_c^2}} - b_0 e \right]^2} \frac{b_0 z^4}{z_c^4} e^{2 - \frac{z^2}{z_c^2}} \quad (4.19)$$

where $\Theta(z)$ is the step function and $\lambda_<(z)$ and $\beta_<(z)$ are the analytical solutions (4.14) and (4.16) of the previous subsection.

We observe that the shapes of the 't Hooft coupling and the beta function are similar to the preceeding case, shown in Figure 1, diverging at $z = z_{max}$.

Depending on n_f , z_{max} can be smaller or larger than z_c . When $z_{max} < z_c$, only the solution $\lambda_<(z)$ is present. This happens when $n_f \leq 2$ (negative c) and $n_f \leq 1$ (positive c). When $z_{max} > z_c$, we have another solution, given by the whole *r.h.s.* of (4.18), and which gives rise to a larger value of z_{max} with respect to the preceding case.

Below, we display in Figure 3 the dependence on λ of the beta function for three values of n_f and the two possible values of c .

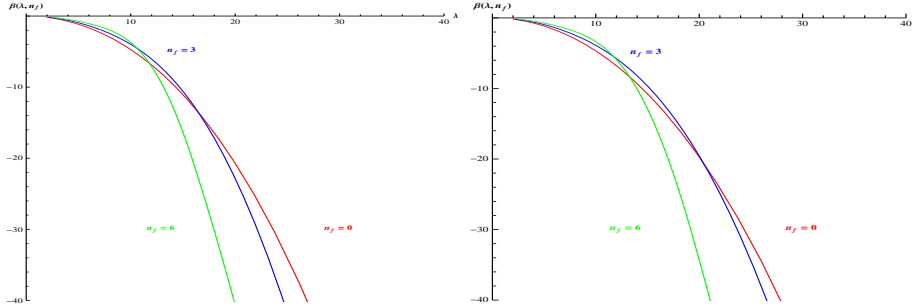


Figure 3: The beta functions $\beta(\lambda)$ as a function of λ for different values of n_f and the two possible values c_{max} (left) and c_{min} (right).

Let us emphasize that changing the sign in (4.13) leads to two different solutions. Nevertheless, the data we have used do not allow us to select a unique beta function.

4.2 Case $k_1^2 < 16k_2$

In this case, the square root on the *r.h.s.* of (4.10) does not vanish for any value of z . Therefore, the upper sign is the only possibility here. Then, we find out:

$$\left(\frac{1}{\lambda} \right)' = -\frac{b_0}{4z} \frac{(\sqrt{4 + k_1 z^2 + k_2 z^4} + \frac{k_1}{4} z^2 + 2) (k_1 + 4\sqrt{k_2})^{\frac{k_1}{4\sqrt{k_2}}}}{(2\sqrt{k_2}\sqrt{4 + k_1 z^2 + k_2 z^4} + 2k_2 z^2 + k_1)^{\frac{k_1}{4\sqrt{k_2}}}} e^{1 - \frac{1}{2}\sqrt{4 + k_1 z^2 + k_2 z^4}} \quad (4.20)$$

which cannot be solved analytically. The parameter c calculated from Eqs.(4.1) and (4.8) with $m = 2$ can assume any value inside the range $c_{min} < c < c_{max}$.

In order to analyse the behaviour of the general equation (4.20), let's write its integral from z to z_0 in the form:

$$\frac{1}{\lambda_0} - \frac{1}{\lambda(z)} = F(z, z_0) . \quad (4.21)$$

Then, the 't Hooft coupling reads

$$\lambda(z) = \frac{\lambda_0}{1 - \lambda_0 F(z, z_0)} . \quad (4.22)$$

For small enough values of n_f , namely $n_f \leq 4$, there is always a $z = z_{max}$ at which $\lambda(z)$ diverges. Moreover, this occurs for any value of c . Then, the shapes of $\lambda(z)$, $\beta(z)$ and $\beta(\lambda)$ are similar to the ones displayed in the Figures 1, 2 and 3.

On the contrary, for $n_f \geq 5$, we will see that the results turn out to be completely different. In the sequel, we will consider the illustrative case $n_f = 6$.

First, we observe that for c close to the extreme values of its allowed range, the coupling solution remains singular. Like the two cases considered above, there is a value $z = z_{max}$ for which the denominator $1 - \lambda_0 F(z_{max}, z_0)$ vanishes.

However, there is an interval for c , namely

$$c \in [-(0.957 \text{ GeV})^2, (0.164 \text{ GeV})^2] , \quad (4.23)$$

for which this denominator never vanishes. As a result, the coupling and the beta function are finite for all z . We show in Figure 4 the behaviour of $1 - \lambda_0 F(z, z_0) = \lambda_0/\lambda(z)$ as a function of z and c .

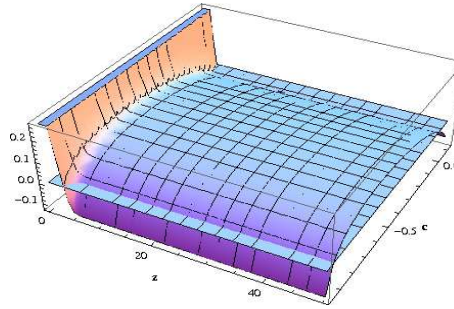


Figure 4: The function $\lambda_0/\lambda(z)$ and the zero-value plane surface. The coordinate z and the parameter c run respectively from 0 to 50 and from its extremal values $c_{min} \simeq -0.966 \text{ GeV}^2$ to $c_{max} \simeq 0.118 \text{ GeV}^2$.

Further, in Figure 5, we show the 't Hooft couplings and the beta functions for some noticeable values of c . The red and green curves correspond to the two limiting values $c = (0.165 \text{ GeV})^2$ and $c = -(0.958 \text{ GeV})^2$ beyond which $\lambda(z)$ and $\beta(z)$ are

singular at z_{max} . On the other hand, for any value of the parameter c inside this interval, the 't Hooft coupling presents an *IR fixed point* λ_* . Accordingly, the beta function *vanishes* for sufficiently large z . Figure 5 also displays the case $c = 0$ (no background dilaton field) and the mid-value $c = -(0.687 \text{ GeV})^2$ as well.

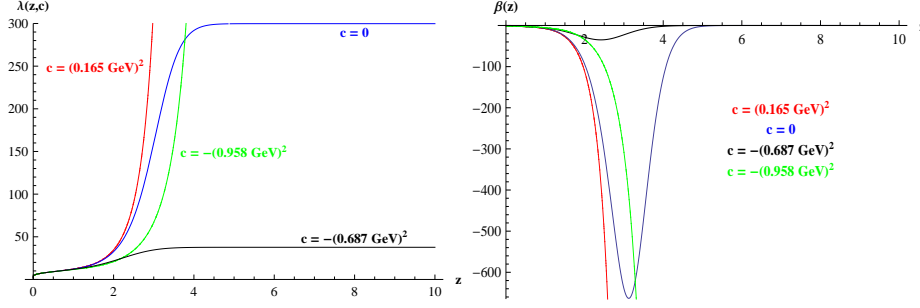


Figure 5: The 't Hooft coupling $\lambda(z)$ and the associated beta function $\beta(z)$ in terms of z for some remarkable values of c in the case $n_f = 6$.

$c \text{ (GeV}^2\text{)}$	$z_{max} \text{ (GeV)}$	λ_*
$(0.165)^2$	4.300	
$(0.164)^2$		61670
0		300
$-(0.686)^2$		38
$-(0.957)^2$		3005
$-(0.958)^2$	4.873	

Table 7: Numerical estimates for z_{max} and λ_* for some values of the dilaton parameter inside the interval (4.23) and immediately beyond.

In Table 7, we list the numerical estimates for z_{max} and λ_* for some characteristic values of c . Note that λ_* takes very different values.

Finally, we plot the beta functions in terms of λ in the Figure 6. Within the interval (4.23), $\beta(\lambda)$ shows the typical behaviour associated with an IR fixed point at finite coupling. On the other hand, for c close to its extremal values, we recover the monotonous decreasing of $\beta(\lambda)$.

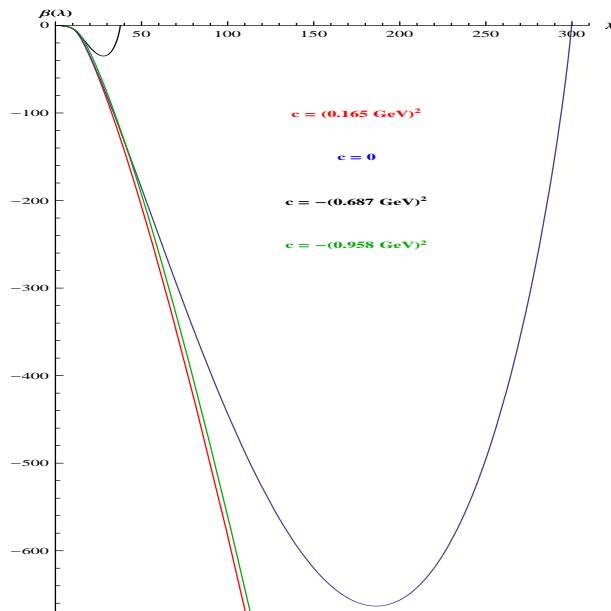


Figure 6: beta functions in terms of λ for $n_f = 6$ and different values of c when $k_1^2 < 16k_2$.

5. Conclusion

The AdS/CFT correspondence provides a well-defined relation between the dimensions of Yang-Mills theory operators and the masses of the corresponding supergravity fields. Nevertheless, for QCD-like gauge theories, the dimensions of operators receive anomalous contributions coming from quantum effects. In this paper, we have developed an extended AdS/QCD approach taking into account the anomalous dimensions of the operators entering the expression of QCD trace anomaly. We considered the scalar glueball spectroscopy within the AdS/QCD Soft-Wall framework. Following this extended model, the mass of the scalar bulk field acquires a dependence on the gauge theory beta function. This modification is then reflected in the eigenvalue equation that determines the $4d$ glueball masses.

We investigated the relation between beta functions and masses in two different (complementary) ways. In Chapter 3, we considered some possible QCD beta functions discussed in the literature and calculated the corresponding glueball mass spectra, comparing with lattice results. For each case, we found ranges of parameters that fit lattice data. Interestingly, some beta functions give rise to the formation of a hard-wall in the $5d$ effective potential.

In Chapter 4, we followed the inverse way: we started from the glueball masses calculated using lattice and found out beta functions that lead to this spectrum. We find different types of beta functions classified according to their IR behaviour. For a class of beta functions, an IR cutoff, z_{max} , which is not present in the Soft-Wall model naturally emerges and gives rise to asymptotically decreasing $\beta(\lambda)$. There is

also another class of beta functions that vanish at large λ , leading to an IR fixed point at finite coupling. The IR vanishing beta functions offer a large range of possible values for the IR fixed coupling.

A better knowledge of mass spectroscopy in different channels would further constrain the holographic parameters. This could help answering the question of the presence or not of an IR fixed point and its value.

Acknowledgments: The authors are partially supported by Capes and CNPq, Brazilian agencies. One of us, F.J., is very grateful to J. A. Helay el-Neto for his kind and invaluable hospitality at the CBPF during the completion of this work.

References

- [1] G. 't Hooft, “A Planar Diagram Theory for Strong Interactions,” Nucl. Phys. B **72**, 461 (1974).
- [2] J. M. Maldacena, “The large N limit of superconformal field theories and supergravity,” Adv. Theor. Math. Phys. **2**, 231 (1998) [Int. J. Theor. Phys. **38**, 1113 (1999)]. [arXiv:hep-th/9711200].
- [3] S. S. Gubser, I. R. Klebanov and A. M. Polyakov, “Gauge theory correlators from non-critical string theory,” Phys. Lett. B **428**, 105 (1998). [arXiv:hep-th/9802109].
- [4] E. Witten, “Anti-de Sitter space and holography,” Adv. Theor. Math. Phys. **2**, 253 (1998). [arXiv:hep-th/9802150].
- [5] J. Polchinski and M. J. Strassler, “Hard scattering and gauge/string duality,” Phys. Rev. Lett. **88**, 031601 (2002) [arXiv:hep-th/0109174].
- [6] V. A. Matveev, R. M. Muradian and A. N. Tavkhelidze, “Automodellism in the large - angle elastic scattering and structure of hadrons,” Lett. Nuovo Cim. **7**, 719 (1973).
- [7] S. J. Brodsky and G. R. Farrar, “Scaling Laws At Large Transverse Momentum,” Phys. Rev. Lett. **31**, 1153 (1973).
- [8] S. J. Brodsky and G. R. Farrar, “Scaling Laws For Large Momentum Transfer Processes,” Phys. Rev. D **11**, 1309 (1975).
- [9] H. Boschi-Filho and N. R. F. Braga, “Gauge/string duality and scalar glueball mass ratios,” JHEP **0305**, 009 (2003) [arXiv:hep-th/0212207].
- [10] H. Boschi-Filho and N. R. F. Braga, “QCD/String holographic mapping and glueball mass spectrum,” Eur. Phys. J. C **32**, 529 (2004) [arXiv:hep-th/0209080].
- [11] G. F. de Teramond & S. J. Brodsky, “The hadronic spectrum of a holographic dual of QCD,” Phys. Rev. Lett. **94**, 201601 (2005) [arXiv:hep-th/0501022].

- [12] A. Karch, E. Katz, D. T. Son and M. A. Stephanov, “Linear confinement and AdS/QCD,” *Phys. Rev. D* **74**, 015005 (2006) [arXiv:hep-ph/0602229].
- [13] P. Colangelo, F. De Fazio, F. Jugeau and S. Nicotri, “On the light glueball spectrum in a holographic description of QCD,” *Phys. Lett. B* **652**, 73 (2007) [arXiv:hep-ph/0703316].
- [14] P. Colangelo, F. De Fazio, F. Jugeau & S. Nicotri, ”Investigating AdS/QCD duality through scalar glueball correlators”, *Int. J. Mod. Phys. A* **24** (2009) 4177-4192 [arXiv:hep-ph/0711.4747].
- [15] P. Colangelo, F. De Fazio, F. Giannuzzi, F. Jugeau & S. Nicotri, ”Light scalar mesons in the soft-wall model of AdS/QCD,” *Phys. Rev. D* **78** (2008) 055009 [arXiv:hep-ph/0807.1054].
- [16] H. Forkel, ”Holographic glueball structure,” *Phys. Rev. D* **78** (2008) 025001 [arXiv:hep-ph/0711.1179].
- [17] U. Gursoy and E. Kiritsis, “Exploring improved holographic theories for QCD: Part I,” *JHEP* **0802**, 032 (2008) [arXiv:0707.1324 [hep-th]].
- [18] U. Gursoy, E. Kiritsis and F. Nitti, “Exploring improved holographic theories for QCD: Part II,” *JHEP* **0802**, 019 (2008) [arXiv:0707.1349 [hep-th]].
- [19] U. Gursoy, E. Kiritsis, L. Mazzanti, G. Michalogiorgakis and F. Nitti, “Improved Holographic QCD,” *Lect. Notes Phys.* **828**, 79 (2011) [arXiv:1006.5461 [hep-th]].
- [20] H. B. Meyer, “Glueball regge trajectories,” hep-lat/0508002.
- [21] C. J. Morningstar and M. J. Peardon, “The Glueball spectrum from an anisotropic lattice study,” *Phys. Rev. D* **60**, 034509 (1999) [hep-lat/9901004].
- [22] Y. Chen, A. Alexandru, S. J. Dong, T. Draper, I. Horvath, F. X. Lee, K. F. Liu and N. Mathur *et al.*, “Glueball spectrum and matrix elements on anisotropic lattices,” *Phys. Rev. D* **73**, 014516 (2006) [hep-lat/0510074].
- [23] B. Lucini and M. Teper, “SU(N) gauge theories in four-dimensions: Exploring the approach to $N = \infty$,” *JHEP* **0106**, 050 (2001) [hep-lat/0103027].
- [24] V. Mathieu, N. Kochelev and V. Vento, “The Physics of Glueballs,” *Int. J. Mod. Phys. E* **18**, 1 (2009) [arXiv:0810.4453 [hep-ph]].
- [25] E. Klempt and A. Zaitsev, “Glueballs, Hybrids, Multiquarks. Experimental facts versus QCD inspired concepts,” *Phys. Rept.* **454**, 1 (2007) [arXiv:0708.4016 [hep-ph]].
- [26] B. Lucini, A. Rago and E. Rinaldi, “Glueball masses in the large N limit,” *JHEP* **1008**, 119 (2010) [arXiv:1007.3879 [hep-lat]].

- [27] L. Susskind and E. Witten, “The Holographic bound in anti-de Sitter space,” hep-th/9805114.
- [28] S. S. Gubser, A. Nellore, S. S. Pufu and F. D. Rocha, “Thermodynamics and bulk viscosity of approximate black hole duals to finite temperature quantum chromodynamics,” Phys. Rev. Lett. **101**, 131601 (2008) [arXiv:0804.1950 [hep-th]].
- [29] D. -f. Zeng, “Heavy quark potentials in some renormalization group revised AdS/QCD models,” Phys. Rev. D **78**, 126006 (2008) [arXiv:0805.2733 [hep-th]].
- [30] J. Alanen and K. Kajantie, “Thermodynamics of a field theory with infrared fixed point from gauge/gravity duality,” Phys. Rev. D **81**, 046003 (2010) [arXiv:0912.4128 [hep-ph]].
- [31] S. Bethke, “The 2009 World Average of $\alpha(s)$,” Eur. Phys. J. C **64**, 689 (2009) [arXiv:0908.1135 [hep-ph]].
- [32] J. Beringer et al. (Particle Data Group), Phys. Rev. D **86**, 010001 (2012).
- [33] T. A. Ryttov and F. Sannino, “Supersymmetry inspired QCD beta function,” Phys. Rev. D **78**, 065001 (2008) [arXiv:0711.3745 [hep-th]].
- [34] G. S. Bali *et al.* [TXL and T(X)L Collaborations], “Static potentials and glueball masses from QCD simulations with Wilson sea quarks,” Phys. Rev. D **62**, 054503 (2000) [hep-lat/0003012].
- [35] C. McNeile *et al.* [UKQCD Collaboration], “Mixing of scalar glueballs and flavor singlet scalar mesons,” Phys. Rev. D **63**, 114503 (2001) [hep-lat/0010019].
- [36] A. Hart *et al.* [UKQCD Collaboration], “On the glueball spectrum in O(a) improved lattice QCD,” Phys. Rev. D **65**, 034502 (2002) [hep-lat/0108022].
- [37] A. Hart *et al.* [UKQCD Collaboration], “A Lattice study of the masses of singlet 0^{++} mesons,” Phys. Rev. D **74**, 114504 (2006) [hep-lat/0608026].